

## Coherent molecular rotations induced by a femtosecond pulse consisting of two orthogonally polarized pulses

Yuichiro Kida,<sup>1</sup> Shin-ichi Zaitsev,<sup>1</sup> and Totaro Imasaka<sup>1,2</sup>

<sup>1</sup>Department of Applied Chemistry, Graduate School of Engineering, Kyushu University, 744, Motoooka, Nishi-ku, Fukuoka 819-0395, Japan

<sup>2</sup>Center for Future Chemistry, Kyushu University, 744, Motoooka, Nishi-ku, Fukuoka 819-0395, Japan

(Received 26 May 2009; published 19 August 2009)

Stimulated Raman scattering induced by a femtosecond pulse formed by two pulses, polarized orthogonally with respect to each other is reported. High-frequency and low-frequency components generated at the center of the pulse through self-phase modulation temporally overlap. The two components induce a coherent molecular rotation through stimulated Raman scattering. The amplitude of this rotation in this way is larger than that of traditional transient stimulated Raman scattering in which linearly, elliptically, and circularly polarized pulses are used.

DOI: [10.1103/PhysRevA.80.021805](https://doi.org/10.1103/PhysRevA.80.021805)

PACS number(s): 42.65.Dr, 42.65.Ky, 42.65.Re

Recent advances in the development of ultrashort laser systems have facilitated various research topics in the field of ultrafast physics and chemistry. One example is in the induction of a coherent molecular rotation by a femtosecond laser pulse and its use for research into the alignment dependence of photoionization [1,2] and high-harmonic generation [3,4]. These studies have given insight into the relationships between optical fields and molecular orbitals in physical processes. Another application of coherent molecular rotations is for the phase modulation of ultraviolet pulses, useful for the subsequent compression of the pulse width [5–7].

Coherent molecular rotation can be induced by impulsive stimulated Raman scattering (ISRS) [8] or transient stimulated Raman scattering (TSRS) [9]. In ISRS, a coherent molecular rotation is induced impulsively using an intense pump pulse whose pulse duration is shorter than the period of a molecular rotation. Although the energy threshold to induce a coherent rotation by ISRS is lower than that by TSRS, a pump pulse shorter than the rotational period of the molecule is required for ISRS [5]. For TSRS on the other hand, the pump pulse does not need to be this short. This method is not as efficient however since the two frequency components for the induction of a coherent rotation is not initially contained in the input pump pulse.

In this Rapid Communication, a way to induce a coherent molecular rotation is discussed. Similar to TSRS, a femtosecond pulse whose pulse duration is longer than the period of a molecular rotation is used to induce the coherent rotation. A pump pulse consisting of a single pulse is used in TSRS, but a pump pulse consisting of two orthogonally polarized pulses is used in the technique. This allows for the induction of a coherent molecular rotation with efficiency higher than TSRS while still using femtosecond pulses whose widths are longer than the period of the rotation.

A femtosecond pulse is passed through a birefringence crystal, and the pulse is split into the ordinary and extraordinary rays (pulses). The two pulses propagate with different group velocities in the crystal, and hence one pulse is temporally delayed with respect to the other when the two pulses emerge from the crystal. The two emerging pulses are or-

thogonally polarized with respect to each other and form a pulse whose polarization changes with time provided that the two pulses are not completely separated from each other. The pulse so formed is hereafter denoted as a polarization-modulated pulse or PM pulse [10,11] as shown in Fig. 1. The polarization variation depends on the phase difference  $\Delta\phi$  between the ordinary and extraordinary rays. For instance, when  $\Delta\phi$  is  $\pi + 2m\pi$  rad, where  $m$  is an integer, any part of the PM pulse is linearly polarized as shown in Fig. 1(b) [11], and we denote the pulse as PM pulse A.

PM pulse A induces a coherent molecular rotation in a regime other than TSRS although the pulse width of the PM pulse is longer than the period of the molecular rotation. When the complex amplitudes of the ordinary and extraordinary rays forming the PM pulse are  $E_o$  and  $E_e$ , respectively, the coupled nonlinear Schrödinger equation describing the interaction between the two rays and a nonlinear medium is expressed as follows:

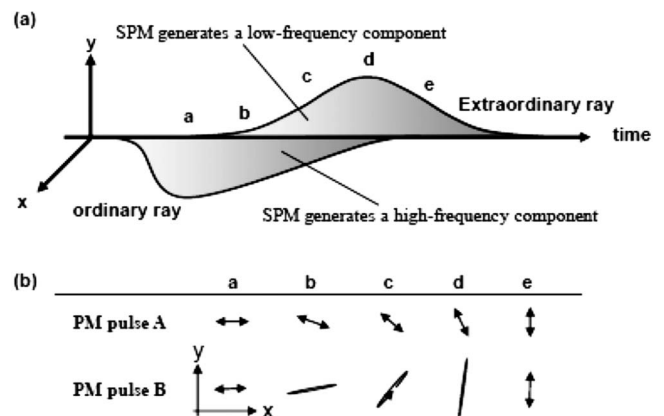


FIG. 1. (a) Temporal distributions of a PM pulse formed by the ordinary and extraordinary rays. The points a, b, c, d, and e indicate the temporal points, and the time separation between the neighboring two points is 63 fs when the PM pulse is generated with a 3-mm-thick  $\text{MgF}_2$  plate. (b) The polarization states of two PM pulses at several temporal points shown in (a).

$$\frac{\partial E_a}{\partial z} + \sum_{k=2} \frac{i^{k-1}}{k!} \left( \frac{\partial^k \beta}{\partial \omega^k} \right)_{\omega=\omega_0} = i \frac{n_2 \omega_0}{c} \left( 1 + \frac{i}{\omega_0} \frac{\partial}{\partial \tau} \right) \left[ \left( |E_a|^2 + \frac{2}{3} |E_b|^2 \right) E_a + \frac{1}{3} E_b^2 E_a^* \right], \quad (1)$$

where the nonlinear polarization arises from self-phase modulation (SPM), cross phase modulation (XPM), four-wave mixing (FWM), and self-steeping (ST) [12]. The terms  $\omega_0$ ,  $\beta$ , and  $n_2$  are, respectively, the carrier angular frequency, propagation constant, and nonlinear-index coefficient for the ordinary and extraordinary rays. The asterisk in the equation designates the complex conjugate, and the symbol  $a$  is  $o$  ( $e$ ) when the symbol  $b$  is  $e$  ( $o$ ). The equation is written under the retarded frame of reference  $(\tau, z)$  propagating with the group velocity of the ordinary or extraordinary ray. The term containing  $|E_a|^2$  in Eq. (1) leads to the modulation of the carrier frequency of the electric field via SPM which broadens the spectral width of the femtosecond pulse and is used to generate few-cycle optical pulses [13]. The spectral broadening by SPM is suppressed partially by XPM, the term containing  $|E_b|^2$  in Eq. (1). This is caused by the two fields of the ordinary ray and the extraordinary ray overlapping in the center of the PM pulse as shown in Fig. 1(a). XPM does not, however, completely suppress the frequency modulation caused by SPM. The nonlinear optical effects arising from terms other than SPM and XPM on the right-hand side of Eq. (1) also have little effect in suppressing this effect. As a result, in the center of the PM pulse, the frequencies of the trailing part of the ordinary ray and the leading part of the extraordinary ray are converted by SPM into frequency components higher and lower than the carrier frequency of the two rays [see Fig. 1(a)], respectively. Since the two frequency components temporally overlap, they induce a coherent molecular rotation through the process of SRS when the frequency difference between the high-frequency and low-frequency components reaches the energy of the Raman shift for a molecular rotation.

The frequency difference depends on the efficiency of the frequency modulation by SPM at the center of the PM pulse and thus depends on the peak intensities of the ordinary and the extraordinary rays forming the PM pulse. When the peak intensities of the two rays are low, the difference between the high-frequency and the low-frequency components generated by SPM is small. In this case, coherent molecular motion with a long motional period is selectively induced. When the

peak intensities of the two rays are high, on the other hand, the frequency difference is large and a coherent molecular motion with a short motional period is also induced. Therefore, coherent molecular motions with several types of periods of molecular motions can be simultaneously induced, in contrast to the conventional TSRS [14].

To estimate the amplitude of the induced coherent molecular rotation induced by a pump pulse (PM pulse), the spectral broadening of a low-intensity probe pulse propagating along with the pump pulse after a certain time delay from the pump pulse is useful [15]. A portion of the energy of the probe pulse is converted into Stokes and anti-Stokes emissions as the result of the phase modulation by the coherent molecular rotation. When the efficiency of the energy conversion is high, the amplitude of the coherent molecular rotation is large. Additionally, the spectrum of the probe pulse after the phase modulation also depends on the angular momentum of the coherent rotation. When clockwise and counterclockwise coherent rotations are simultaneously induced, the energy of a linearly polarized probe pulse is converted into high-order Stokes and anti-Stokes lines, resulting in a broad spectrum [16,17].

In this experiment, a portion of a near-infrared pulse emerging from a chirped-pulse amplifier (100 fs, 784 nm, 1kHz, 1 mJ, horizontally polarized, Concerto, Thales) was split off using a beam splitter and was passed through a half-wave plate followed by a 1.5-mm-thick LiB<sub>3</sub>O<sub>5</sub> (LBO) crystal used to produce an ultraviolet probe pulse polarized horizontally, as shown in Fig. 2. The near-infrared pulse from the beam splitter (pump pulse) was passed through a half-wave plate and a 1-cm-thick polarizer made of calcite to control the energy of the pump pulse. The polarization of the pump pulse was then tilted by 45° to the horizontal axis in the laboratory frame (hereafter denoted as the  $x$  axis) using a half-wave plate. By passing the pump pulse through a quarter-wave plate and a 3-mm-thick MgF<sub>2</sub> plate whose slow axis was along the vertical axis in the laboratory frame (hereafter denoted as the  $y$  axis) and by setting the input angle of the pump pulse into the MgF<sub>2</sub> plate to approximately 16°, the pump pulse was converted into the PM pulse A. After the pump pulse (PM pulse A) and the probe pulse were spatially overlapped using a dichroic mirror, they were focused into a Raman cell (800-mm-long and 5-mm-thick fused silica windows) filled with pressurized hydrogen gas (10 atm) using a fused-silica planoconvex lens with a focal length of 500 mm. The time averaged spectra of the pump and probe pulses emerging from the Raman cell were measured with a multi-channel spectrometer (wavelength resolution of 2.5 nm, spectral range of 300–1100 nm, USB2000, Ocean Optics). The time delay of the probe pulse with respect to the pump pulse in the Raman cell was adjusted at approximately 1 ps at which the spectral modulation of the probe pulse by XPM induced by the pump pulse and the dephasing of the coherent

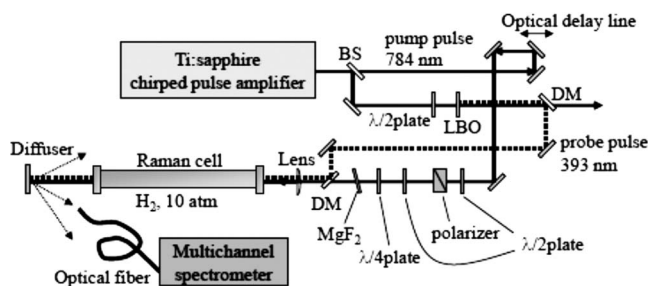


FIG. 2. The experimental setup. BS, beam splitter; DM, dichroic mirror.

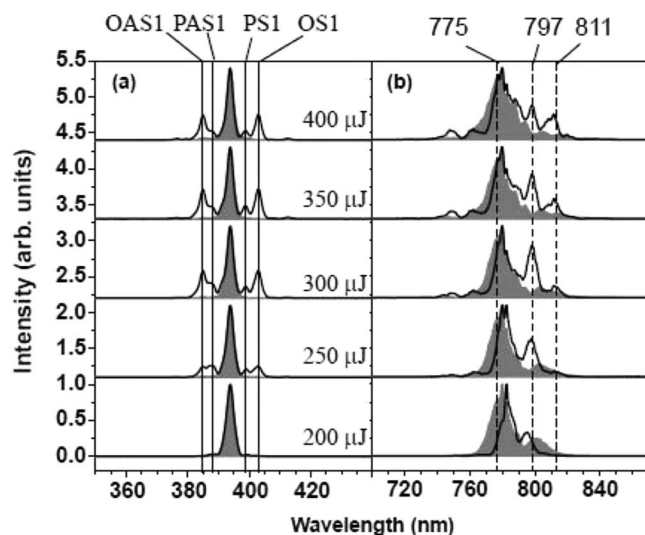


FIG. 3. The spectra of output (a) probe and (b) pump pulses from the Raman cell in the case of the pump pulse of PM pulse A (solid lines) and in the case of the linearly polarized pump pulse (non-PM pulse, shaded curves).

molecular rotation induced by the pump pulse are negligibly small. The energy of the probe pulse in front of the focusing lens was  $10 \mu\text{J}$ .

The spectrum of the output probe pulse from the PM pulse A is shown in Fig. 3(a). The spectral peaks in the vicinity of the fundamental emission line of the probe pulse (393 nm) were generated by the frequency modulation of the parahydrogen (PS1 and PS2) and orthohydrogen (OS1 and OS2). The ratio between the intensities of the peaks arising from orthohydrogen and parahydrogen increased with increasing energy of the pump pulse. At the same time, the intensities of the component at 775 nm and especially the peak at 811 nm contained in the spectrum of the output pump pulse [Fig. 3(b)] increased. This can be explained as follows: the frequency components at 774 and 775 nm in the output spectrum of the pump pulse would be generated at the center of the PM pulse by frequency modulation of the ordinary ray by SPM, while the frequency components at 797 and 811 nm in the output pump pulse would be generated by frequency modulation of the extraordinary ray by SPM. The difference between 774 and 797 nm corresponds to the Raman shift frequency of parahydrogen ( $354 \text{ cm}^{-1}$ ), while the difference between 775 and 811 nm corresponds to that of orthohydrogen ( $587 \text{ cm}^{-1}$ ). Therefore the components at 774 and 797 nm induced the coherent rotation of parahydrogen and the frequency components at 775 and 811 nm induced the coherent rotation of orthohydrogen. In the case of a pump pulse with the energy lower than  $300 \mu\text{J}$ , the efficiency of the SPM was high enough to generate an intense peak at 797 nm but not high enough to generate an intense peak at 811 nm. Therefore, the amplitude of the coherent rotation of orthohydrogen induced by the spectral components at 811 and 775 nm was not large enough to generate spectral sidebands arising from orthohydrogen with intensities higher than those of the sidebands arising from parahydrogen in the spectrum of

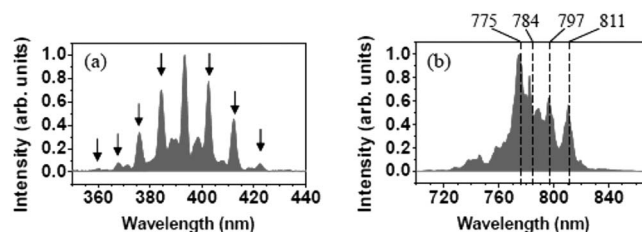


FIG. 4. The spectra of the (a) probe and (b) pump pulses emitted from the Raman cell in the cases of the pump pulse of PM pulse B. Arrows show the Raman emissions arising from orthohydrogen.

the output probe pulse. In the case of a pump pulse with the energy higher than  $300 \mu\text{J}$ , the efficiency of the SPM was high enough for the generation of an intense spectral component at 811 nm. The two spectral components at 775 and 811 nm generated at the center part of the PM pulse A induced stimulated Raman scattering and lead to the amplification of the spectral component at 811 nm. By the amplification process, the amplitude of the coherent rotation of orthohydrogen and the intensities of the corresponding spectral sidebands in the probe pulse [OS1 and OAS1 in Fig. 3(a)] increased with increases in the energy of the pump pulse.

The amplification of the peak at 811 nm and the spectral peaks in the vicinity of the fundamental emission of the probe pulse were not observed, and the frequency of the probe pulse was not modulated when the pump pulse was replaced by a linearly polarized pump pulse (non-PM pulse) as shown in Fig. 3. This was due to the spectral components at 775 and 811 nm which were generated by SPM were not temporally overlapped in the case of the non-PM pulse. In other words, the temporal overlap of the high- and low-frequency components generated by SPM plays a crucial role in the induction of a coherent molecular rotation by PM pulse A.

The efficiency of the induction of a coherent molecular rotation depends on the polarization of the pump pulse as well as the frequency components contained in the pump pulse [18–20]. An elliptically polarized pump pulse can be used to efficiently induce clockwise and counterclockwise coherent molecular rotations [20]. For this reason, an elliptically polarized PM pulse (PM pulses B) with small ellipticity was used, as shown in Fig. 1(b). The amplitude of the ordinary ray contained in PM pulse B was smaller than that of the extraordinary ray. Experimentally, the PM pulse B was produced by tilting the slow axis of the quarter-wave plate by  $10^\circ$  about the  $y$  axis. In addition, the half-wave plate and the polarizer for the energy adjustment were removed which increased the energy of PM pulse B to  $442 \mu\text{J}$ .

The spectra of the output probe pulse and pump pulse (PM pulse B) from the Raman cell are shown in Fig. 4. In the spectrum of the output pump pulse, two intense peaks are generated at 797 and 811 nm [see Fig. 4(b)]. This feature is similar to the output spectrum in the case of the pump pulse of PM pulse A with the energy of  $400 \mu\text{J}$  [Fig. 3(b)]. These spectral peaks were therefore amplified through SRS arising from parahydrogen and orthohydrogen, respectively. Consequently, the output spectrum of the probe pulse consisted of

several sidebands generated by the frequency modulation of the probe pulse by coherent rotations of orthohydrogen and parahydrogen. Generation of the high-order rotational Raman lines indicates the induction of both clockwise and counterclockwise coherent molecular rotations. Up to 78% of the energy of a probe pulse was converted into the spectral sidebands using the PM pulse B. On the other hand, when linearly, elliptically, and circularly polarized non-PM pump pulses have been used, the energy conversion efficiencies have been below 60%. Therefore, the presence of two pulses polarized orthogonally with respect to each other played a crucial role in the induction of a coherent molecular rotation by PM pulse B.

The amplitude and angular momentum of a coherent rotation induced by a PM pulse may also relate to the polarization variation of the PM pulse with respect to time since the amplitude and angular momentum depend on the polarization state of a pump pulse [18,19]. The polarization variation of the PM pulse depends on the efficiency of SPM induced during the beam propagation in the hydrogen gas as well as the properties of the birefringence crystal [21]. The SPM induces frequency chirps in the two pulses forming the PM pulse and changes the time dependence of the ellipticity of the PM pulse. Although the efficiency of the SPM and thus the change in the time dependence of the ellipticity were small in the experiments shown above, the change in the time dependence should be considered in the case of a PM

pulse whose energy is higher than that used in the experiments. In that case, the amplitude and angular momentum of a coherent molecular rotation induced by the PM pulse may also depend on the energy of the PM pulse, and high energy-conversion efficiency from a probe pulse into spectral sidebands might be achieved by use of a PM pulse other than PM pulse B.

In summary, a PM pulse consisting of two orthogonally polarized pulses has been used to induce a coherent molecular rotation. During the propagation of a PM pulse through a Raman active medium, high-frequency and low-frequency components are generated by SPM. The two frequency components temporally overlap and induce SRS, resulting in a coherent molecular rotation with amplitudes larger than that induced by traditional TSRS. This technique can also be used for the induction of a coherent molecular vibration, such as coherent vibration of hydrogen molecules, which has a vibrational period of 8 fs. This is not easy using ISRS, where few-cycle pulses are required.

This work was supported by a Grant-in-Aid for the Japan Society for the Promotion of Science (JSPS) Foundation (Project No. 06J09678), Grant-in-Aid for Scientific Research, and a Grant-in-Aid for the Global COE program, "Science for Future Molecular Systems," from the Ministry of Education, Culture, Science, Sports and Technology of Japan.

- 
- [1] I. V. Litvinyuk, K. F. Lee, P. W. Dooley, D. M. Rayner, D. M. Villeneuve, and P. B. Corkum, *Phys. Rev. Lett.* **90**, 233003 (2003).
  - [2] D. Pinkham and R. R. Jones, *Phys. Rev. A* **72**, 023418 (2005).
  - [3] R. Velotta, N. Hay, M. B. Mason, M. Castillejo, and J. P. Marangos, *Phys. Rev. Lett.* **87**, 183901 (2001).
  - [4] J. Itatani, J. Levesque, D. Zeidler, H. Niikura, H. Pépin, J. C. Kieffer, P. B. Corkum, and D. M. Villeneuve, *Nature (London)* **432**, 867 (2004).
  - [5] M. Wittmann, A. Nazarkin, and G. Korn, *Opt. Lett.* **26**, 298 (2001).
  - [6] N. Zhavoronkov and G. Korn, *Phys. Rev. Lett.* **88**, 203901 (2002).
  - [7] Y. Kida, S. I. Zaitzu, and T. Imasaka, *Opt. Express* **16**, 13492 (2008).
  - [8] Y. X. Yan, E. B. Camble, and K. Nelson, *J. Chem. Phys.* **83**, 5391 (1985).
  - [9] A. Laubereau and W. Kaiser, *Rev. Mod. Phys.* **50**, 607 (1978).
  - [10] I. J. Sola, E. Mével, L. Elouga, E. Constant, V. Strelkov, L. Poletto, P. Villoresi, E. Benedetti, J.-P. Caumes, S. Stagira, C. Vozzi, G. Sansone, and M. Nisoli, *Nat. Phys.* **2**, 319 (2006).
  - [11] Y. Kida, S. I. Zaitzu, and T. Imasaka, *Phys. Rev. A* **77**, 063802 (2008).
  - [12] G. P. Agrawal, *Nonlinear Fiber Optics*, 4th ed. (Academic, San Diego, 2006), p. 180.
  - [13] R. L. Fork, C. H. Brito Cruz, P. C. Becker, and C. V. Shank, *Opt. Lett.* **12**, 483 (1987).
  - [14] H. Kawano, Y. Hirakawa, and T. Imasaka, *IEEE J. Quantum Electron.* **34**, 260 (1998).
  - [15] M. Wittmann, A. Nazarkin, and G. Korn, *Appl. Phys. B: Lasers Opt.* **70**, S261 (2000).
  - [16] H. Kawano, A. Suda, and K. Midorikawa, *Appl. Phys. B: Lasers Opt.* **74**, S103 (2002).
  - [17] H. Kawano, K. Ishikawa, A. Suda, and K. Midorikawa, *Opt. Lett.* **27**, 1917 (2002).
  - [18] R. W. Minck, E. H. Hagenlocker, and W. G. Rado, *Phys. Rev. Lett.* **17**, 229 (1966).
  - [19] R. Holmes and A. Flusberg, *Phys. Rev. A* **37**, 1588 (1988).
  - [20] K. Ishikawa, H. Kawano, and K. Midorikawa, *Phys. Rev. A* **66**, 031802(R) (2002).
  - [21] C. Altucci, R. Esposito, V. Tosa, and R. Velotta, *Opt. Lett.* **33**, 2943 (2008).